EasyChair Preprint

№ 2777

Spectroscopic Studies of Li-Ion Battery

Sikander Azam

February 26, 2020

Spectroscopic Studies of Li-Ion Battery

Sikander Azam

Department of Physics Riphah International University Sector I-14 Islamabad, Pakistan.

Abstract

The electronic structure and optical properties of Li-NiO_2 compound has been calculated by means of DFT calculations. The calculated electronic band structures exhibit that the metallic nature with the bands crosses the Fermi, with Ni-d and O p-states overlapping around Fermi level. The anisotropic characteristics of real and imaginary parts of the refractive indices, dielctric function, extension coefficient and energy loss function corresponding to the electric field parallel and perpendicular to the c-axis are studied.

Introduction

In the 20^{th} century, due to high power densities and energy, combustion engine has chiefly powered up the mobility. Burning of hydrocarbons was the major source of transportation in the beginning of 21th century, but due to harm of global warming and their limited supply requires permanent substitute. The substitutes to combustion engine were the electrochemical energy transformation and storage tools like fuel cells and batteries respectively. Recently, in electric and hybrid electric vehicles battery technology has been made for commercial use. Among all these battery technologies, the technology of Lithium-ion (Li-ion) battery technology develops highest potential and advance storage of clean electricity for electrical vehicles, but the main disadvantage of this technique is that it is only suitable for high power appliances [1]. Due to their high power charging interval is small, which is only a fractional part of those thinking of a switch for conversion of a vehicle based on combustion power to an electric vehicle. Due to high power density of Li-ion battery, charging time will be decreased. By multiplying voltage to specific current specific power is obtained. It also depends on the nature of material; selection of appropriate material tends to increased voltage and increased charging/discharging time. By using nanoparticles instead of traditional micro particles of positive electrode material, electrode/electrolyte interface area has been increased remarkably which improves charging/discharging rates [2].

Although a promise was made for increased power density, in Li-ion batteries the use of nanoparticles as active material has not been completely implemented yet. Globally and commercially usage of nanoparticles will need more cleaned electrode formulation and a good understanding about the nature of charge storage. That's why it is directed by the need of better understanding of nanoparticles for their use in Li-ion batteries.

TiO_2 is proposed as exemplary material to complete this crystal because it produce no side reaction within its voltage range. However, TiO_2 nano particles are not used as negative material for commercial interest because of its higher voltage as compared with graphite. After the formulation of electrode, an appropriate method must be established to generate nano particles.

Flame Spray Pyrolysis (FSP) method is used for fabrication, because its process is fast and completed in one step [3, 4]. The positive materials LiV_3O_8, V_2O_5, $LiMn_2O_4$, and carbon/ $LiMn_2O_4$ mixtures were generated by using FSP method. After the generation of these materials, at different charge/discharge rate the findings of electrochemical energy storage are mentioned.

In Li-ion battery charge storage develops positive electrode material which is basically developed as lithium ion insertion/extraction reactions and specific charge is also developed at the active material/electrolyte interface in double layer. The increased form of charge can also be appeared which can be prescribed as self-capacitance [5], and it is very important in nano particles to store the charge. The type of charge storage depends upon how Li-ion injected and differs from Li-ion interpolation that either the charge is stored in the form of absorption on the surface or within the material, rather within the material near the surface. When the average particle diameter is less than 10nm it plays private role. Another important feature of this work is to find out the electrochemical properties of positive electrode material by using cyclic voltammetry, potentiostatic intermittent titration technique and electrochemical impedance spectroscopy and rate capacity experiments.

The main objective of this work is that to find of the drawbacks of using nano particles as active material in Li-ion batteries. The hindrance in the formation of electrode material is also important part of this work. To point out the difficulties in the fabrication of material, investigation of material and electrochemical properties is also main cause of

this work. It will definitely take part in the development of high powered devices such as EV/HEV and many other similar electrochemical devices.

3.2 Calculation Methodology

The crystal structure for Li-NiO_2 compound is depicted in Fig.1.This compound has tetragonal symmetry having space group ofI4/mmm. The optical properties, electronic structure and thermoelectric properties were calculated with the help of full potential linearized augmented plane wave (FPLAPW) technique, as implemented in the Wien2k code [10,11], based on density functional theory (DFT) [12] within local density approximation (LDA) [13], generalized gradient approximation (GGA-PBE) [14], and Engel-Vosko generalized gradient approximation(GGA) [15]and exchange correlation potential. By using spherical polar harmonic functions, the Kohn–Sham wave functions were expanded within the non-overlapping muffin-tin (MT) spheres and by Fourier series in the interstitial region. To obtain the convergence for energy eigen values, the wave functions in the interstitial regions were expanded in the plane waves for the cut off $K_{MAX} \times R_{MT}$ = 7. For Li, Ni and O atoms, the value for muffin-tin radii were chosen exactly to be 2.0 a.u.159**k**-points in the irreducible wedge of the simple tetragonal Brillion zone were taken.

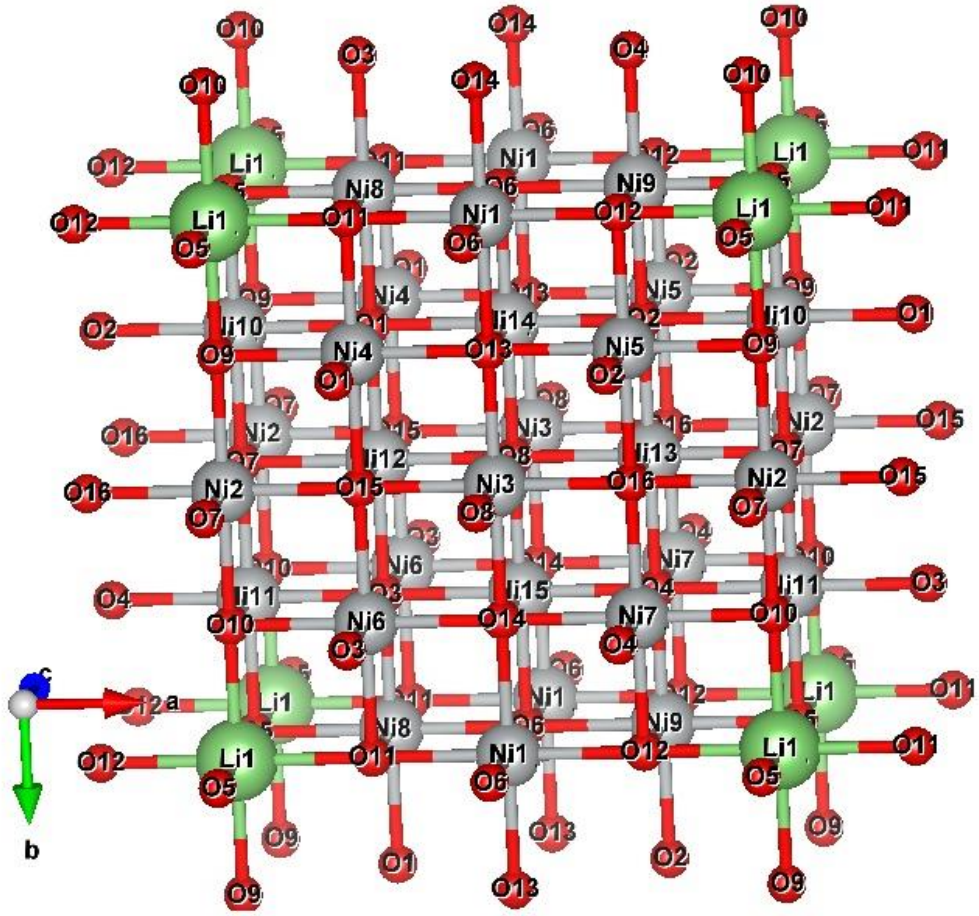

Figure 3.1 2x2x2 Super Cell of Li-NiO_2

3.3. Result and Discussions

3.3.1 Band Structure and Density of States (DOS)

By means of LDA and GGA approximations, we have calculated the electronic band structure, total and partial density of states of the given sample. it is generally known that these approaches have much simpler forms and are not sufficiently flexible to accurately regenerate both the exchange–correlation energy and its charge derivative. Engel and Vosko [15] taking into account this drawback they reconstructed a new functional form of GGA that has the better ability to reproduce the exchange correlation potential at the cost of less agreement in the exchange energy. This new approach, called EV-GGA, provides better band splitting and some other properties that chiefly depend on the accuracy of the exchange–correlation potential. Therefore, we have opted to display the

results obtained by EV-GGA for further interpretation and demonstrating the effect of doping of Li on the electronic structure and the relevant physical properties [16-21].

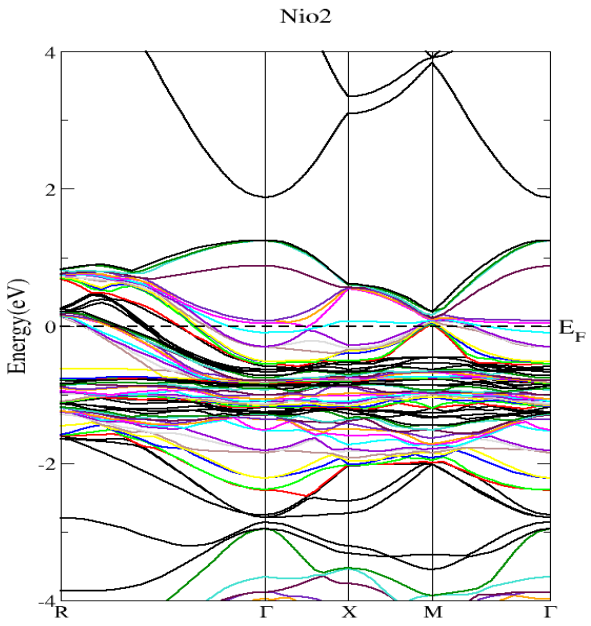

Figure 3.2 Electronic Band Structures of Li doped NiO_2

Figure 3.2 show the electronic band structure of Li doped NiO_2 compound along with the high symmetry points in the Brillouin zone. The computed electronic band structures reveal the metallic nature of the compounds with bands crossing the Fermi level (E_F).To best of our knowledge, there is no experimental data on the band structure of these three compounds is available in the literatures to make a meaningful comparison with our results, but because of successful application of FP-LAPW methods, now we can elaborate the function of the energy band structures for these existing material under the umbrella of present work. Similarly Fig. 2 also shoes that, the bands located around the Fermi levels are because of the admixture of Ni-d and O p-states.

To minutely investigate the nature of the electronic bands structure, we have calculated the total and partial density of states of the given material as shown in Fig. 3. The TDOS and PDOS (Fig. 3a, b, c)vary from -20.0 eV to 14.0 eV; but as we are interested in the optical properties of the Li doped NiO_2 material So, here in we have shown the PDOS from -6.0 to 10.0 eV, (i) from -6.0 eV to -4.0eV the O-p and Ni-d states shows significant

contribution comparatively than the Ni-s/p states. (ii) from -3.0 eV to 1.0 eV, again the major contribution comes from the Ni-d and o-p states but the only difference between the different energies states is that at the lower valance shell the major contribution comes from the O-p states while at the higher valance states the major contributions comes from the Ni- d state.

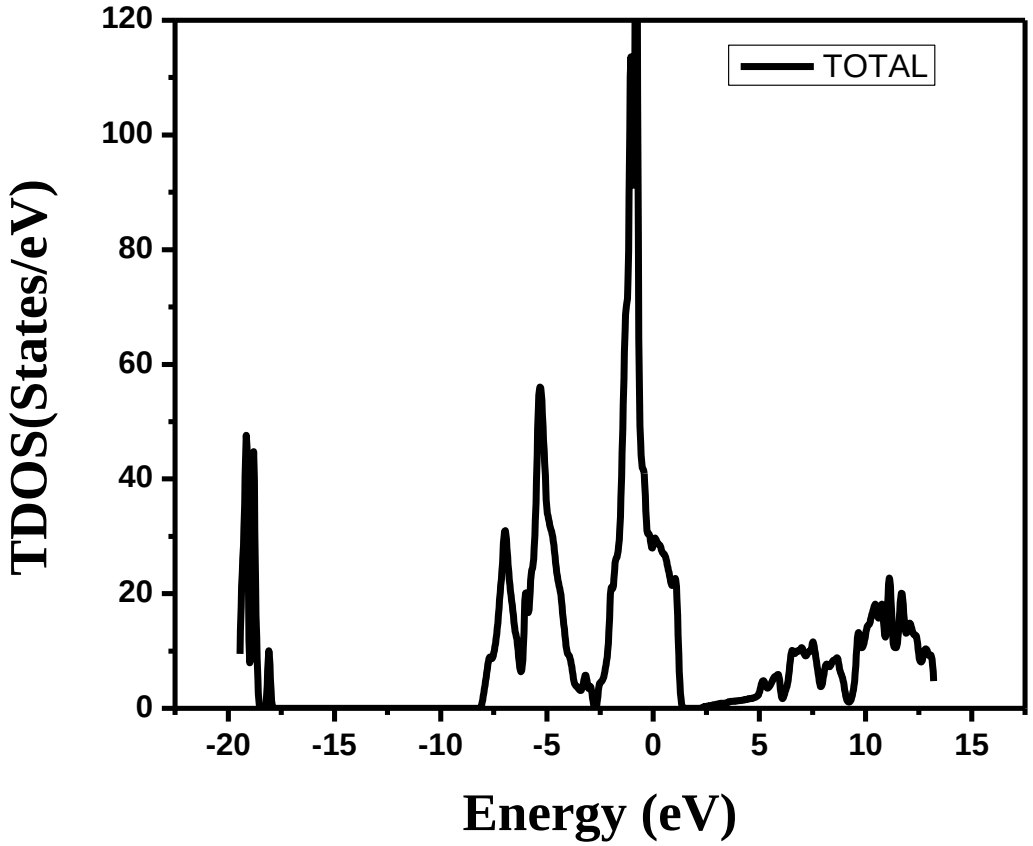

Figure 3.3 Total Density of States (TDOS)

However, the bands lying above and close to the E_F play a prominent role in the properties of materials. Especially, the bands near to E_F are very essential for both phonons and phonon-electron interactions. A strong hybridization exists between Ni-s/p/d and O-s/p states.

The value of total DOS at Fermi level $N(E_F)$ is of the order of 25.0.The finite DOS at the Fermi level clearly show the metallic nature of the material. The density of states

dependent function i.e. the electronic specific heat coefficient γ can be calculated using the expression given below [22-27]

$$\gamma = \frac{1}{3}\pi^2 \mathrm{N}(\mathrm{E}_F) K_\beta^2$$

Where $N(E_F)$= DOS at E_F

and k_B = Boltzmann constant. The calculated density of states at the Fermi energy $N(E_F)$ enables us to calculate the bare electronic specific heat coefficient that is 2.60.

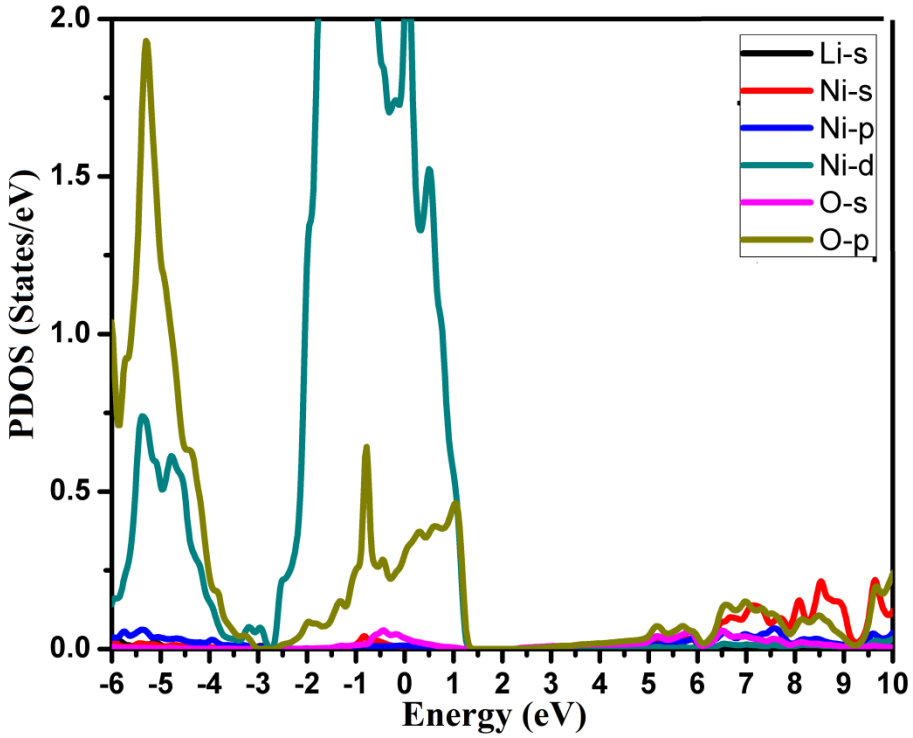

Figure 3.4 Partial Density of States (PDOS)

3.3.2 Optical Properties

A strong comprehension of the electronic structures can be derived by looking into the optical spectra that supplies enough items of information about the occupied and unoccupied states, along with the features of the bands [29, 30]. Optical spectroscopy analysis is a pivotal means to substantiate the overall band behavior of a solid [31]. Optical properties of solids call for the strikingly significant topics, in both rudimentary exploration and for industrial usage. In this regard, the origin and nature of different excitation processes is of fundamental interest, while for the industrial usage, it can be

utilized in many opto-electronic gadgets. Density Functional Theory (DFT) is the endeavoring method for the calculation of materials properties of solids.

The characteristics (lattice) such as lattice parameters, equilibrium volumes, phonon frequencies, atomic positions and elastic constants differ from their experimental values by a few percent only. However, such ground state properties, which rely on the calculation of the total energy, are expressed very trust worthy. By the treatment of excited states, the results are not so bonafied. The prime causes are that the Hohenberg–Kohn theorem only fits for the ground states, and the Kohn–Sham Eigen states should not be interpreted as single-electron states.

Fig. 5 explains the imaginary behavior of the dielectric function of three compounds. As the examined compounds are metallic in nature so we have to take into account the intra-band transitions (Drude term). [32]

$$\varepsilon_2(\omega) = \varepsilon_{2\mathrm{inter}}(\omega) + \varepsilon_{2\mathrm{intra}}(\omega)$$

Where

$$\varepsilon_{2\mathrm{intra}}(\omega) = \frac{\omega_P^2 \tau}{\omega\left(1+\omega^2\tau^2\right)}$$

Where ω_p =mean plasma frequency

And τ = mean free time respectively among the collisions [33] usually expressed as:

$$\omega_p^2 = \frac{8\pi}{3}\sum_{kn} \vartheta^2{}_{kn}\,\delta(\varepsilon_{kn})$$

Where ε_{kn} is $\mathrm{E}_n(k) - \mathrm{E}_F$ and ϑ_{kn} is the velocity of electron in the squared. The effect of Drude term is more substantial for less than 1.0 eV.

To calculate the frequency-dependent dielectric function, the energy eigen values and electron wave function are needed. [34-36].All optical spectra, specifically real and imaginary parts of the dielectric function and reflectivity are studied.

Since the Li doped NiO_2compound has a tetragonal symmetry, thus the dielectric functions are $\varepsilon^{xx}(\omega) = \varepsilon^{yy}(\omega)$ and $\varepsilon^{zz}(\omega)$. The dielectric functions $\varepsilon_2^{xx}(\omega)$, and $\varepsilon_2^{zz}(\omega)$of the investigated compounds [38-40] using the EVGGA are illustrated in Fig. 3.6.

There exists anisotropy between $\varepsilon_2^{xx}(\omega)$ and $\varepsilon_2^{zz}(\omega)$ components. We should emphasize that the $\varepsilon_2^{xx}(\omega)$ component is the dominant.

From the the real parts $\varepsilon_1^{xx}(\omega)$ and $\varepsilon_1^{zz}(\omega)$shown in figure 3.5 and imaginary part of dielectric functions [41] $\varepsilon_2^{xx}(\omega)$ and $\varepsilon_2^{zz}(\omega)$shown in Fig. 3.6 are calculated using the Kramer's–Kronig relations [42]. The results of $\varepsilon_1^{xx}(\omega)$ and $\varepsilon_1^{zz}(\omega)$are shown in figure 3.5. It is clear that there is weak anisotropy between these two components of the frequency-dependent dielectric function [43-45].

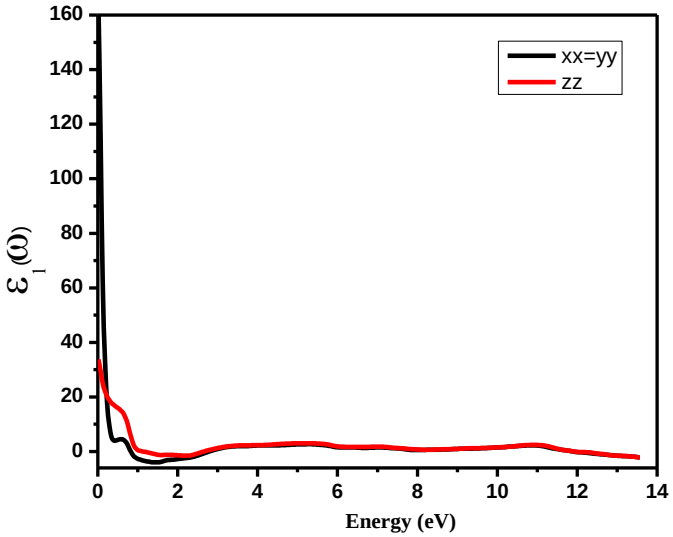

Figure 3.5 Dielectric Function (Real Part)

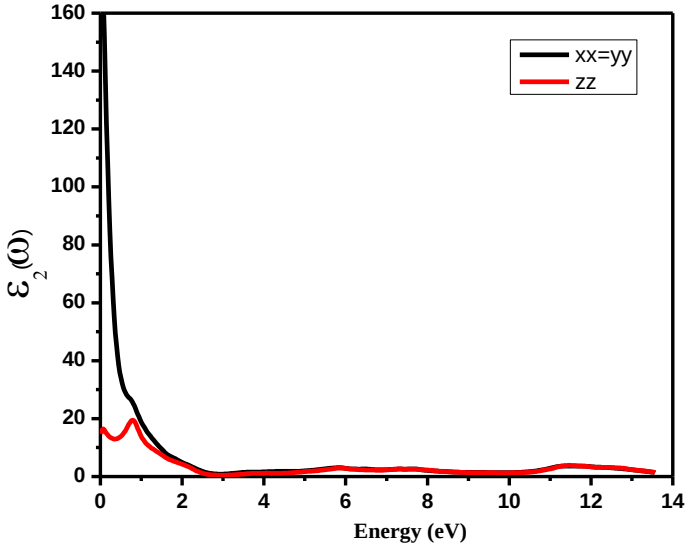

Figure 3.6 Dielectric Function (Imaginary Part)

In Fig. 3.7, the spectra of the electron energy loss function [46] $L^{xx}(\omega)$ and $L^{zz}(\omega)$ have been shown. The electron energy loss function describing the energy loss of a fast moving electron passing through a material is frequently huge at the plasma frequency [47]. Prominent peaks are found at 11.5 to 13.0 eV, which specify decrease in the reflectance.

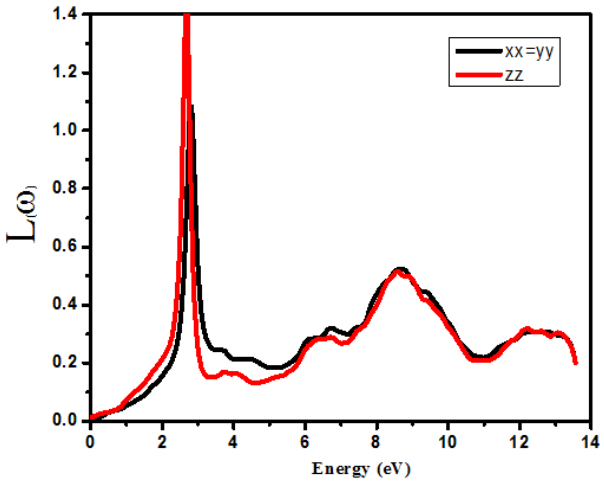

Figure 3.7 Energy Loss Function (L(ω))

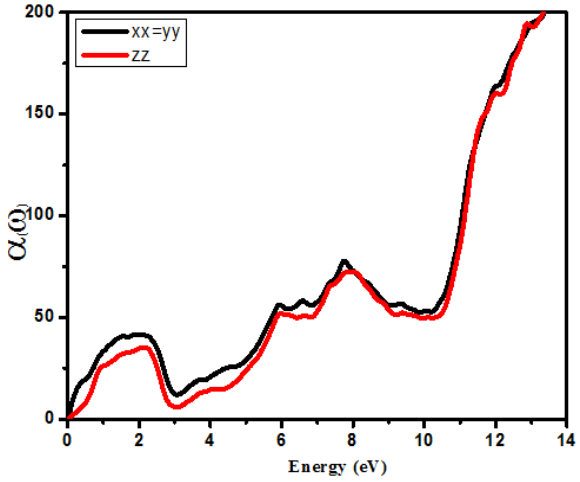

Figure 3.8 Absorption Spectra α(ω)

Calculated absorption spectra for Li doped NiO_2 has been shown in Fig. 3.8.From absorption spectra, it is clear that material is good for absorption of Photons for all ranges of Energy and material shows isotropic behaviour i.e it has same characteristics in all directions. We can see that our material shows variation in absorption spectra from 0eV

to higher values of energy. Further, graph illustrate that material shows minimum absorption at 3 eV while it sharply rises as energy exceeds 11 eV. Hence we can conclude that material is suitable for absorption at higher values of energy.

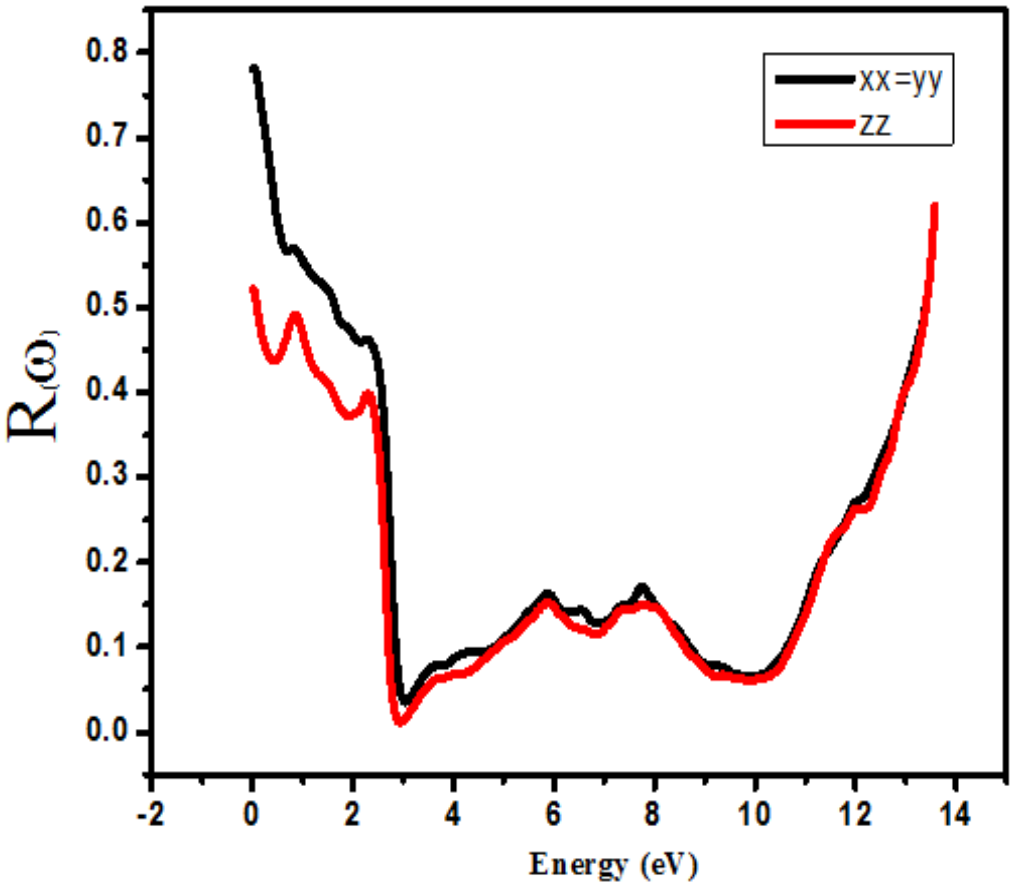

Figure 3.9 Reflectivity Spectra R(ω)

Fig. 3.9, shows the reflectivity spectra $R^{xx}(\omega)$ and $R^{zz}(\omega)$ for the investigated compounds. The reflectivity spectra [48] for all the compounds shows almost the same behavior. But the reflectivity spectra for the $R^{xx}(\omega)$ is a little higher than the other two compounds. From the reflectivity spectra it is clear, that in the energy limit (2.0 to 8.0 eV) shows small reflectivity. This implies that the material is not a good reflector. The energy >2.0 eV and <8.0 eV shows greater reflectivity [49-50] of the compound which means that these material at the specific energies can be used as Bragg reflector [51-52].

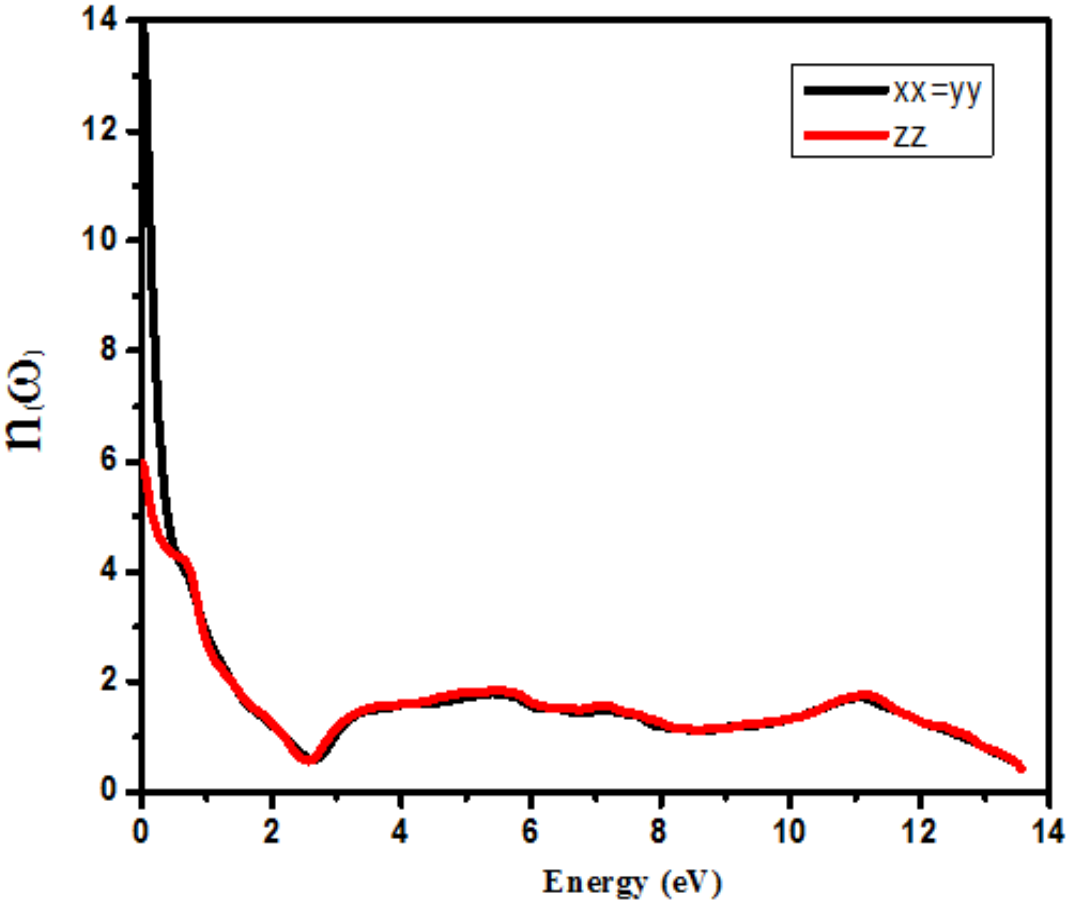

Figure 3.10 Refractive Index Spectra n(ω)

Graph of the refractive index n(ω) verses the photon's energy in a region up to 14.0 eV, represent in Figure 3.10. The refractive index n(ω) of a crystal is directly related to the electronic polarizability of ion and the local fields interior the crystals. The dispersion curve of refractive index has reached its maximum value at 0 eV and then the curves shows sudden decrease at 2.8 eV then, roughly speaking; it shows almost constant behavior from 2.8 eV to 11 eV. As we further increase the energy it goes to n(ω)=0 as we reached at very high enerhy i.e 14 eV. Since peaks in the graph are not enough, it show that it might be a non-transparent material in the visible region, anyhow it shows some transparency for some values in UV region. At zero energy, $n(0)$ which is a significant optical constant have maximum value i.e 14 for x & y axis and that of 6 for z axis.

3.4 Conclusions

In the present work a DFT calculation is performed on Li doped NiO_2 compound. The calculated electronic band structures confirm the metallic nature with the bands crossing the Fermi. The Ni-d and O-p states dominate the Fermi level. The calculated density of states at Fermi level $N(E_F)$ is 25.0, and the bare electronic specific heat coefficient, is found to be 2.60 mJ/mol-K^2.

The frequency dependent optical properties are investigated, which suggest that the investigated compound has preeminent photoelectric properties and can be used in opto-electronic device. The reflectivity spectra show strong reflection in infra-red region.

References

[1] G. K.H. Madsen and D. J. Singh. BoltzTrap. a code for calculating bandstructure dependant quantities. Computer Physics Communications, 175:67, 2006.

[2] M. Born and J.R. Oppenheimer. Zur quantentheorie der molekeln. Annalen der Physik, 380:457, 1927.

[3] R. M. Martin. Electronic structure: Basic Theory and Pratical Methods. Cambridge University Press, 2004.

[4] P. Ghosez. First-principle study of the dielectric and dynamical properties of baryum titanate. Ph.D. thesis, Universit´e catholique de Louvain, 1997.

[5] S. H. Vosko, L. Wilk, and M. Nusair. Accurate spin-dependent electron liquid correlation energies for local spin-density calculations - a critical analysis. Canadian Journal of Physics, 58:1200, 1980.

[6] J. P. Perdew and A. Zunger. Self-interaction correction to density-functional approximations for many-electron systems. Physical Review B, 23:5048, 1981.

[7] J. P. Perdew, K. Burke, and M. Ernzerhof. Generalized gradient approximation made simple. Physical Review Letters, 77:3865, 1996.

[8] P. Ziesche and H. Eschrig. Electronic structure of solids 91, 1991.

[9] A. D. Becke and E. R. Johnson, J. Chem. 124, 221101 (2006) bibitemP. A. M. Dirac1930 P. A. M. Dirac, Proc. Cambridge Philos. Soc. 26 376,(1930)

[10] F. Tran and P. Blaha, Phys. Rev. Lett. 102, 226401 (2009)

[11] A. D. Becke and E. R. Johnson, J. Chem. 124, 221101 (2006) bibitemP. A. M. Dirac1930 P. A. M. Dirac, Proc. Cambridge Philos. Soc. 26 376,(1930)